UCLA
UCLA Previously Published Works

Title

Unusual Enantiodivergence in Chiral Brønsted Acid-Catalyzed Asymmetric Allylation with β-Alkenyl Allylic Boronates

Permalink

https://escholarship.org/uc/item/71s3n2jt

Journal

Angewandte Chemie International Edition, 61(41)

ISSN

1433-7851

Authors

Gao, Shang
Duan, Meng
Andreola, Laura R
et al.

Publication Date

2022-10-10

DOI

10.1002/anie.202208908

Peer reviewed

Unusual Enantiodivergence in Chiral Brønsted Acid-Catalyzed Asymmetric Allylation with β-Alkenyl Allylic Boronates

Shang Gao[+],

Department of Chemistry and Biochemistry, Auburn University, Auburn, AL 36849 (USA)

China Pharmaceutical University, Nanjing, 210009 (China)

Meng Duan[+],

Department of Chemistry and Biochemistry, University of California, Los Angeles, Los Angeles, CA 90095 (USA)

Department of Chemistry and Shenzhen Grubbs Institute, Southern University of Science and Technology, Shenzhen, 518055 (China)

Laura R. Andreola,

Department of Chemistry, University of Georgia, Athens, GA 30602 (USA)

Peiyuan Yu,

Department of Chemistry and Shenzhen Grubbs Institute, Southern University of Science and Technology, Shenzhen, 518055 (China)

Steven E. Wheeler,

Department of Chemistry, University of Georgia, Athens, GA 30602 (USA)

Kendall N. Houk[*],

Department of Chemistry and Biochemistry, University of California, Los Angeles, Los Angeles, CA 90095 (USA)

Ming Chen[*]

Department of Chemistry and Biochemistry, Auburn University, Auburn, AL 36849 (USA)

Abstract

We report herein a rare example of enantiodivergent aldehyde addition with β-alkenyl allylic boronates via chiral Brønsted acid catalysis. 2,6-Di-9-anthracenyl-substituted chiral phosphoric acid-catalyzed asymmetric allylation using β-vinyl substituted allylic boronate gave alcohols with *R* absolute configuration. The sense of asymmetric induction of the catalyst in these reactions is opposite to those in prior reports. Moreover, in the presence of the same acid catalyst, the reactions with β-2-propenyl substituted allylic boronate generated homoallylic alcohol products with *S* absolute configuration. Unusual substrate-catalyst C–H⋯π interactions in the favoured

[*] mzc0102@auburn.edu, houk@chem.ucla.edu.
[+] These authors contributed equally to this work.

Conflict of Interest

The authors declare no conflict of interest.

reaction transition state were identified as the origins of observed enantiodivergence through DFT computational studies.

Keywords

Boronates; C–H···π Interactions; Chiral Phosphoric Acids; Enantiodivergence; Organocatalysis

Introduction

Asymmetric catalysis has significantly accrued importance in organic chemistry over the past three decades, as it becomes one of the most adopted approaches to synthesize chiral nonracemic molecules.[1,2] Among available tactics, asymmetric catalysis via biological molecules, transition metal complexes and small organic molecules have garnered the most attention. In vast majority of the enzymatic catalysis, however, minor perturbations to the substrate structures often have profound influences on chemical reactivities of the reactant, and perhaps more importantly, the optical purities of the reaction product. By contrast, asymmetric catalysis with transition metal complexes or small organic molecules are much more promiscuous toward the substrate or reagent structural variations. It is generally true that these processes can tolerate substrates or reagents with considerable structural differences to generate chiral products with comparable enantioselectivities. And enantiomeric products can normally be created from reactions with the antipode of the catalyst separately.

Pioneered independently by the Akiyama and Terada groups,[3] BINOL-derived chiral phosphoric acids are a class of small molecule organic catalysts that have been widely exploited in asymmetric catalysis.[4] In particular, the ease for modifying the substituents at the 3- and 3'-positions of the BINOL backbone has facilitated the development of a variety of acid catalysts with different electronic and steric properties. The mode of catalysis of chiral phosphoric acids typically involves a hydrogen-bonding network between the acid catalyst and the substrate. The chiral information from the resulting catalyst-substrate complex often dictates the formation of one enantiomer product selectively. By taking advantage of this novel mode of catalysis, a broad range of asymmetric transformations have been developed during the past 20 years using these small molecule catalysts.[4] In particular, several chiral phosphoric acids have exhibited excellent levels of asymmetric induction in aldehyde addition with allylboronates to generate highly enantioenriched homoallylic alcohols.[5] Owing to the exceptional fidelity of asymmetric induction from these catalysts, the reactions have been successfully extended to a wide range of unsaturated organoboron compounds.[6–9]

In connection to an ongoing synthesis project, we became interested in developing catalytic asymmetric methods that allow for the access to enantioenriched homoallylic alcohols bearing an alkene group at the γ-position, **2** and **4** (Scheme 1).[10] Such alcohols are key structural motifs in several members of the amphidinolide natural product family.[11,12] Moreover, the diene moieties of **2** and **4** can participate in a variety of transformations to generate important building blocks for complex molecule syntheses.[13] As illustrated

in Scheme 1, a chiral Brønsted acid-catalyzed aldehyde allylation approach is envisioned to produce enantioenriched homoallylic alcohols **2** and **4**. Accordingly, we report herein the discovery of chiral phosphoric acid-catalyzed enantiodivergent aldehyde addition with β-alkenyl allylboronates. In the presence of a catalytic amount of acid (*S*)-**A₂**, asymmetric addition to aldehydes with boronate **1a** formed enantioenriched alcohols **2** with *R* absolute configuration, which is opposite to the sense of asymmetric induction of the catalyst as shown in prior allylation studies. On the other hand, the reactions of boronate **3** with the same acid catalyst afforded alcohols **4** with *S* absolute configuration. It is particularly striking that, in the presence of the same acid catalyst (*S*)-**A₂**, a small structural variation of boron reagents **1a** and **3** (a methyl group) led to the formation of alcohol products with opposite configuration. This serendipitous discovery provides a rare example of enantiodivergent catalysis by chiral phosphoric acids.[14]

Results and Discussion

We began our studies by developing suitable conditions for asymmetric addition to benzaldehyde with pinacol boronate **1a**. Following the initial report from the Antilla group,[5a] chiral phosphoric acid (*S*)-**A₁** (TRIP) has been employed to catalyze asymmetric aldehyde addition with a wide array of allyl,[6] allenyl,[7] and propargyl boronates[8] to form highly enantioenriched alcohol products. Therefore, we anticipated acid (*S*)-**A₁** should catalyze the reaction of boronate **1a** with benzaldehyde to give product (*S*)-**2a** with high enantiopurity.[9] When **1a** (1.2 equiv) was treated with benzaldehyde at –45 °C in the presence of 5 mol% of acid (*S*)-**A₁**, alcohol (*S*)-**2a** was obtained in 86% yield, albeit with only 79:21 er. It has been shown that the diol motif on boron could drastically influence the enantioselectivities of the reactions.[8b,15] We were intrigued whether the enantioselectivity could be improved by modifying the diol unit of boron reagent **1a**. Toward this end, we prepared a small collection of boronates **1b**–**f** and conducted reactions of benzaldehyde with **1b**–**f** in the presence of acid catalyst (*S*)-**A₁**. Much to our dismay, while the yields of product **2a** were high, the enantioselectivities of these reactions were not improved. The enantiomeric ratios of product (*S*)-**2a** range from 79:21 er to 55:45 er, with the one from the reaction with pinacol boronate **1a** being the best (Table 1).

Besides (*S*)-**A₁**, several other chiral phosphoric acids have been shown to catalyze asymmetric aldehyde addition to form alcohol products with excellent optical purities. [5b,c,8b] To explore whether the structures of chiral phosphoric acids could impact enantioselectivities of the reaction, several catalysts (*S*)-**A₁**–**A₈** were evaluated for the reactions of **1a** with benzaldehyde. As illustrated in Table 2, while the reaction with acid (*S*)-**A₁** as the catalyst gave alcohol (*S*)-**2a** in 79:21 er, the reaction with 9-anthracyl-substituted acid (*S*)-**A₂** afforded product **2a** in 90:10 er, strikingly, with (*R*)-**2a** as the major enantiomer (entry 2, Table 2). In accord with mechanistic studies from prior chiral phosphoric acid-catalyzed asymmetric aldehyde allylboration,[5,9] enantiomer (*S*)-**2a** should be formed selectively with (*S*)-**A₂** as the catalyst. However, we consistently obtained the same results after conducting the reaction several times with acid catalyst (*S*)-**A₂** from different commercial sources. Given the high fidelity of asymmetric induction[5,6] in chiral phosphoric acid-catalyzed allyl addition reactions, it is completely unexpected that acids

(*S*)-**A₁** and (*S*)-**A₂**, which bear the same chiral (*S*)-BINOL backbone, afforded opposite enantiomers of product **2a**. Intriguingly, acid catalysts with other aromatic groups such as 9-phenanthrenyl [(*S*)-**A₃**] or 1-pyrenyl [(*S*)-**A₄**] only gave near racemic product **2a** (entries 3 and 4). To probe whether such phenomena are true for chiral phosphoric acids with other backbones, we conducted the reactions with (*S*)-**A₅** or (*S*)-**A₆** as the catalyst, both of which have an H_8-BINOL unit. As we surmised, the reaction with (*S*)-**A₅** as the catalyst, which is closely related to (*S*)-**A₁** (TRIP), gave (*S*)-**2a** (84:16 er) as the major enantiomer (entry 5). By contrast, the reaction with acid (*S*)-**A₆**, which resembles (*S*)-**A₂**, produced enantiomer (*R*)-**2a** (77:23 er) preferentially (entry 6). The same trend was observed again for the reactions with catalysts (*S*)-**A₇** and (*S*)-**A₈**, both possessing an identical SPINOL backbone. While (*S*)-**2a** (81:19 er) was formed as the major enantiomer with catalyst (*S*)-**A₇** (entry 7), the reaction with acid (*S*)-**A₈** as the catalyst delivered (*R*)-**2a** in 76:24 er (entry 8). Among these acids we evaluated, the reaction with (*S*)-**A₂** was the most enantioselective. Final tweak of the reaction conditions revealed that 4 Å molecular sieves are important to the enantioselectivity of the reaction (entry 9). A slight boost of the optical purity of (*R*)-**2a** was achieved with (*S*)-**A₂** as the catalyst when the reaction was conducted in a 1:1 toluene and cyclohexane mixed solvent system (entry 10). These results indicate that the reactions selectively generated the (*S*)-enantiomer of **2a** when acid (*S*)-**A₁**, (*S*)-**A₅**, or (*S*)-**A₇** bearing a 2,4,6-triisopropyl-phenyl group was employed as the catalyst. On the other hand, the reactions with acid (*S*)-**A₂**, (*S*)-**A₆**, or (*S*)-**A₈**, which has a 9-anthracyl group, preferred forming enantiomer (*R*)-**2a** selectively.

The general applicability of the reaction is summarized in Table 3. A variety of aldehydes participated in the reaction to give alcohols (*R*)-**2** in 72–98% yields with 90:10 to 98:2 er. To confirm the *R* absolute configuration of the hydroxyl group in **2**, modified Mosher ester analyses were conducted with several representative alcohols **2** (bottom panel, Table 3).[16] The results are fully consistent with assigned *R* configuration of the hydroxyl group in alcohols **2**. Moreover, X-ray crystallography analyses of compounds **2f**, **2i**, **2j** and **2k** further corroborated the *R* absolute configuration of hydroxyl group. To the best of our knowledge, such a chiral phosphoric acid-catalyzed asymmetric allylation that produces opposite enantiomers from acid catalysts bearing the same chiral backbone has not been documented in any prior literature.[17] It is apparent that the steric model established by the Goodman group is not operational in this case.[9a] A new mode of catalysis is likely involved in these reactions.

To investigate whether the observed enantiodivergence with catalysts (*S*)-**A₁** and (*S*)-**A₂** is applicable to other systems, we evaluated asymmetric aldehyde addition with several other unsaturated boronates. As shown in Scheme 2, the reaction of allylboronate **5** with benzaldehyde in the presence of acid (*S*)-**A₁** produced homoallylic alcohol **6** in 88% yield with 98:2 er. When acid (*S*)-**A₂** was employed, the same alcohol **6** was obtained in 93% yield with a lower enantiomeric ratio (82:18). In both cases, the major enantiomer product **6** has the same configuration. The reactions of γ-ethoxy-*E*-allylboronate **7** with either acid catalyst (*S*)-**A₁** or (*S*)-**A₂** also gave identical product **8** with comparable enantioselectivities.[18] The same trend was observed again in reactions with propargylic boronate **9**, both delivering alcohol **10** with similar enantiomeric purities.[8b] For reactions

with allenyl boronate **11**, homopropargylic alcohol **12** obtained via catalyst (*S*)-**A$_1$** is highly enantioenriched (95:5 er).[7a] When acid (*S*)-**A$_2$** was employed, much lower ee was observed for alcohol **12** (67:33 er). Nevertheless, the major enantiomers from these two reactions share the same absolute configuration. However, we discovered that the reactions of allenyl boronate **13** employing acid (*S*)-**A$_1$** as the catalyst afforded homopropargylic alcohols **14** (97:3 er) and **15** (98:2 er) with *S* configuration.[7e] By contrast, the enantiomeric products, *ent*-**14** (80:20 er) and *ent*-**15** (81:19 er) with *R* absolute configuration, were isolated in the reactions with acid (*S*)-**A$_2$** as the catalyst. Among all examined boron reagents, only reactions with the methyl-substituted allenyl boronate **13** exhibited a similar enantiodivergence behavior to the reactions with **1a**. Again, it is intriguing that the trends of enantioselection in the reactions with allenyl boronates **11** and **13** are drastically different, given the small structural difference between the two boron reagents.

Enantioenriched alcohols **4** are valuable intermediates in organic synthesis. Methods that allow for highly enantioselective preparation of such molecules are rare.[13a] We were intrigued whether the reaction could be extended to boron reagent **3**, as it could readily provide the access to chiral nonracemic alcohols **4** (Scheme 3). Based on the results in Tables 2–3, it was expected that acid (*S*)-**A$_2$**-catalyzed reaction of aldehydes with reagent **3** should form alcohols (*R*)-**4** selectively. As shown in Scheme 3, when reagent **3** was treated with benzaldehyde at −45 °C in the presence of acid (*S*)-**A$_1$**, alcohol **4a** was obtained in 87% yield with 78:22 er. The *S* absolute configuration of major enantiomer (*S*)-**4a** is consistent with the sense of asymmetric induction of acid catalyst (*S*)-**A$_1$** in prior reports (also see the results of reagent **1a** with acid (*S*)-**A$_1$** as the catalyst shown Table 1). When the reaction of **3** was conducted with acid (*S*)-**A$_2$** as the catalyst, product **4a** was isolated in 90% yield in 91:9 er, surprisingly, also with the *S* absolute configuration. Mosher ester analyses of **4a** further confirmed the *S* absolute configuration of the hydroxyl group.[16] It is apparent that the major enantiomers obtained from these two reactions with reagent **3** share the same *S* configuration, regardless of the structures of the acid catalysts (*S*)-**A$_1$** and (*S*)-**A$_2$**.

Table 4 summarizes the scope of aldehyde in reactions with reagent **3** in the presence of acid catalyst (*S*)-**A$_2$**. Alcohol products (*S*)-**4a**–**i** were isolated in 76–99% yields with 91:9 to 96:4 er. The *S* absolute configuration of the hydroxyl group was established by Mosher ester analyses of several representative alcohols **4**.[16] The X-ray crystallography analyses of compounds **4b**, **4e** and **4f** further confirmed the absolute configuration. It is remarkable that, even though the only difference between two boronate reagents, **1a** and **3**, is a methyl group, acid (*S*)-**A$_2$**-catalyzed reactions with these two reagents gave alcohols (*R*)-**2** and (*S*)-**4** with opposite absolute configuration (Tables 3 and 4). Again, these data point to potential different modes of catalysis of acid (*S*)-**A$_2$** in reactions with reagents **1a** and **3**.

Adducts **2** and **4** obtained from these reactions contain a diene unit, which can undergo various chemical transformations. As shown in Scheme 4, Cu-catalyzed protoboration of the mono-substituted alkene unit of **2a** gave boronate **16** in moderate yield. Alternatively, protection of the hydroxyl group of **2a** gave TBS-ether **17**, which underwent the same protoboration process to afford boronate **18** in 86% yield. Diene **17** participated in Pt-catalyzed 1,4-diboration at 80 °C to deliver boronate **19** in 87% yield.[19] Cobalt-catalyzed

coupling of diene **17** with ethyl acrylate gave skipped diene **20** in 83% yield with 16:1 *E*-selectivity at the methyl-substituted olefin group.[20] Subsequent DBU-promoted alkene isomerization of **20** produced conjugated diene **21** with > 30:1 *Z*-selectivity. The alkene geometry of **20** and **21** was assigned by nOe studies. In addition, [4+2] cycloaddition of the diene group of **17** with dimethyl acetylenedi-carboxylate followed by DDQ-mediated aromatization gave product **22** in 92% yield.[21] 1,4-Diboration of TBS-ether **23** was also conducted, affording diboronate **24** in 92% yield. Lastly, the diene group of **23** participated in La(OTf)$_3$-catalyzed [4+2] cycloaddition with diethyl azodicarboxylate to give tetrahydropyridazine **25** in 95% yield.[22]

Computational Studies

To elucidate the origins of observed enantiodivergence in the chiral phosphoric acid (*S*)-**A$_1$** and (*S*)-**A$_2$**-catalyzed aldehyde addition with boronate **1a**, and to investigate the origins of the asymmetric induction in (*S*)-**A$_2$**-catalyzed reactions with reagent **1a**, density functional theory (DFT) calculations were performed using Gaussian 16.[23] At the theoretical level, geometries were optimized at B3LYP/6–31G(d), and single-point energies and solvent effects were investigated at M06–2X/6–311+G(d,p)-CPCM (toluene).[24] Thermochemistries were corrected with the Head-Gordon and Grimme corrections using GoodVibes version 3.0.1, with quasiharmonic approximations to entropy and enthalpy and corrected for 228.15 K.[25] Conformation searches were conducted using the CREST conformer-rotamer ensemble sampling tool version 2.10.2 with xtb version 6.3.3.[26]

Two different catalysis models, reported by the Goodman and Houk groups, were utilized for computational studies.[7a,9a,b] As shown in Figure 1, in the Goodman model, the chiral phosphoric acid catalyst forms a ternary complex with the aldehyde and allylboronate. The competing reaction transition states feature a bidentate chelate via hydrogen bonding of the acid catalyst with the hydrogen atom of the aldehyde and the axially positioned oxygen atom of the boronate. In the Houk model, the chiral phosphoric acid coordinates to the equatorially oriented oxygen atom of the boron reagent, and the phosphoryl oxygen interacts with one hydrogen atom of the phenyl group in reaction transition states. On the basis of prior reports on chiral phosphoric acid (*S*)-**A$_1$**-catalyzed allylboration reactions, the most favorable transition state, **TS-ax**, involves the *si*-face addition to benzaldehyde via the axial model, which leads to the formation of major enantiomer (*S*)-**6**.[5,9] Meanwhile, the lowest energy transition state (**TS-eq**) delivering the minor enantiomer (*R*)-**6** corresponds to the equatorial model, with the allylboronate attacking the *re*-face of benzaldehyde.

To gain insights into the roles of 3- and 3'-substituents of phosphoric acid catalysts in determining the enantioselectivity of aldehyde addition with reagent **1a**, computational studies on acid (*S*)-**A$_1$**-catalyzed reaction of benzaldehyde with boronate **1a** were performed first. The reaction formed a pair of enantiomers, (*R*)-**2a** and (*S*)-**2a**, in a 21:79 ratio, favoring enantiomer (*S*)-**2a** (entry 1, Table 1). As shown in Figure 2, for the *re*-face attack that leads to minor enantiomer (*R*)-**2a**, transition state **TS-1-eq** via the equatorial model is preferred to transition state **TS-1-ax** via the axial model by 2.0 kcal mol^{-1}. Meanwhile, transition state **TS-2-ax**, featuring the *si*-face attack via the axial model to give (*S*)-**2a**, is found to be 1.0 kcal mol^{-1} lower in energy than transition state **TS-1-eq**. The energy

difference between **TS-1-eq** and **TS-2-ax** is in good agreement with the enantioselectivity observed experimentally (21:79 er). Moreover, formation of (*S*)-**2a** as the major enantiomer is consistent with the sense of asymmetric induction of (*S*)-**A$_1$** in all prior reports on chiral phosphoric acid (*S*)-**A$_1$**-catalyzed aldehyde allylboration reactions (More details are given in Supporting Information, Figure S1 and the accompanying discussions).[5,6]

Next, DFT calculations on chiral phosphoric acid (*S*)-**A$_2$**-catalyzed benzaldehyde addition with boron reagent **1a** were conducted. In this reaction, alcohol (*R*)-**2a** was obtained as the major enantiomer in 90:10 er (entry 2, Table 2). As illustrated in Figure 3, the calculations revealed that transition state **TS-3-ax** via the axial model, which features a *re*-face attack to give (*R*)-**2a**, is 4.1 kcal mol^{-1} more favorable in energy than transition state **TS-3-eq** via the equatorial model (which also delivers (*R*)-**2a**). This finding is in sharp contrast to the results obtained from the calculations on (*S*)-**A$_1$**-catalzed *re*-face addition to benzaldehyde with **1a**, where transition state **TS-1-eq** via the equatorial model is energetically more favorable than transition state **TS-1-ax** via the axial model. Moreover, transition state **TS-3-ax** (*re*-face attack) is calculated to be1.2 kcal mol^{-1} more favorable than transition state **TS-4-ax** (*si*-face attack). This finding is in good accord with the experimentally observed enantiomeric excess of (*R*)-**2a** (90:10 er). The results indicate that substituting the 2,4,6-triisopropylphenyl group with a 9-anthracyl group in the catalyst completely alters the enantioselection of the reaction.

To probe the origins of energy difference between reaction transition states **TS-3-eq** and **TS-3-ax** with the 9-anthracyl group in the catalyst, non-covalent interaction (NCI) analyses were conducted (Figure 4).[27] The independent gradient model (IGM) was chosen due to its ability to extract intermolecular NCIs. The calculations indicate there is no apparent steric difference in transition states **TS-3-eq** and **TS-3-ax**. However, the key difference between the two transition structures is the position of the β-vinyl group of boronate **1a**. In disfavored transition state **TS-3-eq**, the vinyl group of boronate **1a** points away from the anthracyl group of the acid catalyst. By contrast, it parallels to the anthracyl group in favored transition state **TS-3-ax** (shown as the large green discs, Figure 4), suggesting the presence of strong C–H···π interactions in transition state **TS-3-ax**. Further calculations were performed by replacing the vinyl group of **1a** with a hydrogen atom then calculating the single-point without optimization. The energy difference between two competing transition states decreased to 0.4 kcal mol^{-1}, which is significantly smaller than the one between **TS-3-eq** and **TS-3-ax** (4.1 kcal mol^{-1}). These data suggest that the attractive C–H···π interactions between the vinyl group and the anthracyl group are likely responsible for the preference of transition state **TS-3-ax** over **TS-3-eq** in chiral phosphoric acid (*S*)-**A$_2$**-catalyzed aldehyde addition with reagent **1a**.

To clarify the factors that control the enantioselectivity in acid (*S*)-**A$_2$**-catalyzed reaction with reagent **1a**, where **TS-3-ax** is more favorable than transition state **TS-4-ax** by1.2 kcal mol^{-1}, the distortion/interaction analyses of the transition states were carried out.[28] The geometries of transition states **TS-3-ax** and **TS-4-ax** are divided into two fragments: the acid catalyst and boronate-benzaldehyde complex. According to the calculations, the distortion energy difference of acid catalyst and boronate-benzaldehyde complex between

TS-4-ax and **TS-3-ax** is –0.7 and 0.2 kcal mol^{-1}, respectively. On the other hand, the computed interaction energy favors **TS-3-ax** by 2.4 kcal mol^{-1} over **TS-4-ax**. Therefore, the total energy of **TS-4-ax** is1.9 kcal mol^{-1} higher than **TS-3-ax** using distortion/interaction analyses. Inspection of the optimized geometries by NCI analyses confirms that the origins of difference in interaction energy are mainly due to the C–H⋯π interactions (Figure 4). In the favored transition state **TS-3-ax**, the vinyl group of **1a** interacts more strongly with the anthracyl group of catalyst (*S*)-**A$_2$** (shown as the large green discs in **TS-3-ax**, Figure 4). By contrast, in the disfavored transition state **TS-4-ax**, the vinyl group is positioned into the narrow pocket of the acid catalyst. Such an arrangement leads to the vinyl group adopting a T-shape conformation with the anthracyl group of (*S*)-**A$_2$**, which results in much weaker C–H⋯π interactions (shown as the small green discs in **TS-4-ax**, Figure 4). Therefore, transition state **TS-3-ax** features much stronger C–H⋯π interactions between reagent **1a** and acid catalyst (*S*)-**A$_2$**. Moreover, single-point calculations were conducted by replacing the vinyl group of boronate **1a** with a hydrogen atom (Figure 4). The energy difference between two competing transition states decreases to –0.9 kcal mol^{-1}, which again suggests the difference of C–H⋯π interactions in transition states **TS-3-ax** and **TS-4-ax** of (*S*)-**A$_2$**-catalyzed reaction with reagent **1a** is the crucial contributor to the observed enantioselectivity. It is worth noting that such C–H⋯π interactions have not been documented in prior phosphoric acid-catalyzed aldehyde addition with unsaturated organoboron compounds. This serendipitous discovery could be valuable for the design of novel chiral phosphoric acid catalysts that exploit such C–H⋯π interactions.

As shown in Table 4, the reactions between aldehydes and reagent **3** with phosphoric acid (*S*)-**A$_2$** as the catalyst provided alcohols (*S*)-**4** as the major enantiomers of the reactions. The sense of asymmetric induction of acid (*S*)-**A$_2$** in these reactions is the same as those with acid (*S*)-**A$_1$** as the catalyst (Scheme 3). However, such sense of asymmetric induction is opposite to the one from reactions with reagent **1a** (Table 3), even the same catalyst (*S*)-**A$_2$** was employed in these reactions. To probe the origins of observed enantioselectivities in these reactions, theoretical studies were conducted on the reaction between boronate **3** and benzaldehyde with acid (*S*)-**A$_2$** as the catalyst. As depicted in Figure 5, transition state **TS-5-ax** with the *re*-face attack on benzaldehyde is calculated to be 2.0 kcal mol^{-1} less favorable compared to transition state **TS-6-ax** with the *si*-face attack. The reaction via the lower energy transition state, **TS-6-ax**, gave product (*S*)-**4a** as the major enantiomer, which is consistent with the experimental results. Closely examining the optimized geometry of **TS-5-ax** revealed that the methyl group of boronate **3** is oriented toward the narrow pocket of acid catalyst (*S*)-**A$_2$**, which results in weak C–H⋯π interactions (shown as the small green discs in **TS-5-ax**, Figure 5, bottom panel). Moreover, this orientation results in the absence of stabilizing C–H⋯O=P hydrogen-bonding interactions between the phenyl hydrogen and phosphoryl oxygen of the catalyst, which further destabilizes transition state **TS-5-ax**. By contrast, transition state **TS-6-ax** exhibits the attractive C–H⋯O=P hydrogen-bonding interaction in addition to strong C–H⋯π interactions, which ultimately makes **TS-6-ax** the favored transition state in the reaction with reagent **3**. Overall, chiral phosphoric acid (*S*)-**A$_2$**-catalyzed aldehyde addition with boronate **3** proceeds through the energetically more favorable **TS-6-ax** to afford product **4a** with *S* absolute configuration. This analysis is consistent with the experimental observation.

Conclusion

In summary, we report our serendipitous findings on the enantiodivergence of chiral Brønsted acid-catalyzed allylation. With the same acid catalyst (*S*)-**A₂**, the reactions of aldehydes with β-vinyl substituted allylboronate **1a** gave alcohol products **2** with *R* absolute configuration as the major enantiomer, while the reactions with a structurally closely related reagent, β–2-propenyl substituted allylboronate **3**, generated *S*-enantiomers of alcohol products **4** preferentially.[29] Moreover, in reactions with reagent **1a**, the sense of asymmetric induction of acid catalyst (*S*)-**A₂** is opposite to those in prior reports.[30] Such discrepancy in enantioselectivities and asymmetric induction has not been disclosed in any chiral phosphoric acid-catalyzed asymmetric aldehyde addition reactions. DFT computational studies were conducted to probe the origins of observed enantiodivergence. Unusual C–H···π interactions between the boron reagent **1a** and the catalyst (*S*)-**A₂** were identified as the dominant contributor to the observed enantioselectivities. These results could be highly valuable for the development of novel chiral phosphoric acid catalysts by exploiting the C–H···π interactions as part of the design elements.

Supplementary Material

Refer to Web version on PubMed Central for supplementary material.

Acknowledgements

Data Availability Statement

The data that support the findings of this study are available in the supplementary material of this article.

References

[1]. a)Jacobsen EN, Pfaltz A, Yamamoto H, Comprehensive Asymmetric Catalysis, Vols. I–III, Suppl. I–II, Springer, New York, 1999;b)Ojima I, Catalytic Asymmetric Synthesis, 2nd ed., Wiley-VCH, Weinheim, 2000;c)Carreira EM, Yamamoto H, Comprehensive Chirality, Vols. 1–9, Elsevier, Amsterdam, 2012.

[2]. a)Hawkins JM, Watson TJN, Angew. Chem. Int. Ed 2004, 43, 3224;Angew. Chem 2004, 116, 3286;b)Farina V, Reeves JT, Senanayake CH, Song JJ, Chem. Rev 2006, 106, 2734. [PubMed: 16836298]

[3]. a)Akiyama T, Itoh J, Yokota K, Fuchibe K, Angew. Chem. Int. Ed 2004, 43, 1566;Angew. Chem 2004, 116, 1592;b)Uraguchi D, Terada M, J. Am. Chem. Soc 2004, 126, 5356. [PubMed: 15113196]

[4]. a)Akiyama T, Chem. Rev 2007, 107, 5744; [PubMed: 17983247] b)Terada M, Chem. Commun 2008, 4097;c)Akiyama T, Mori K, Chem. Rev 2015, 115, 9277; [PubMed: 26182163] d)Parmar D, Sugiono E, Raja S, Rueping M, Chem. Rev 2014, 114, 9047. [PubMed: 25203602]

[5]. a)Jain P, Antilla JC, J. Am. Chem. Soc 2010, 132, 11884; [PubMed: 20690662] b)Barrio P, Rodríguez E, Saito K, Fustero S, Akiyama T, Chem. Commun 2015, 51, 5246;c)Xing C-H, Liao Y-X, Zhang Y, Sabarova D, Bassous M, Hu Q-S, Eur. J. Org. Chem 2012, 1115.

[6]. a)Miura T, Nishida Y, Morimoto M, Murakami M, J. Am. Chem. Soc 2013, 135, 11497; [PubMed: 23886015] b)Incerti-Pradillos CA, Kabeshov MA, Malkov AV, Angew. Chem. Int. Ed 2013, 52, 5338;Angew. Chem 2013, 125, 5446;c)Huang Y, Yang X, Lv Z, Cai C, Kai C, Pei Y, Feng Y, Angew. Chem. Int. Ed 2015, 54, 7299;Angew. Chem 2015, 127, 7407;d)Miura T, Nakahashi J, Murakami M, Angew. Chem. Int. Ed 2017, 56, 6989;Angew. Chem 2017, 129, 7093;e)Miura T, Nakahashi J,Zhou W, Shiratori Y, Stewart SG, Murakami M, J. Am. Chem. Soc 2017, 139, 10903; [PubMed: 28708391] f)Miura T, Oku N, Murakami M, Angew. Chem. Int. Ed 2019, 58, 14620;Angew. Chem 2019, 131, 14762;g)Gao S, Chen M, Org. Lett 2020, 22, 400; [PubMed: 31869238] h)Chen J, Chen M, Org. Lett 2020, 22, 7321; [PubMed: 32903009] i)Liu J, Chen M, Org. Lett 2020, 22, 8967; [PubMed: 33125249] j)Gao S, Duan M, Shao Q, Houk KN, Chen M, J. Am. Chem. Soc 2020, 142, 18355; [PubMed: 33052047] k)Miura T, Oku N, Shiratori Y, Nagata Y, Murakami M, Chem. Eur. J 2021, 27, 3861; [PubMed: 33277755] l)Gao S, Liu J, Chen M, Chem. Sci 2021, 12, 13398; [PubMed: 34777758] m)Gao S, Duan M, Liu J,Yu P, Houk KN, Chen M, Angew. Chem. Int. Ed 2021, 60, 24096;Angew. Chem 2021, 133, 24298.

[7]. a)Jain P, Wang H, Houk KN, Antilla JC, Angew. Chem. Int. Ed 2012, 51, 1391;Angew. Chem 2012, 124, 1420;b)Reddy LR, Org. Lett 2012, 14, 1142; [PubMed: 22273041] c)Chen M, Roush WR, J. Am. Chem. Soc 2012, 134, 10947; [PubMed: 22731887] d)Tsai AS, Chen M,Roush WR, Org. Lett 2013, 15, 1568; [PubMed: 23484801] e)Wang M, Khan S,Miliordos E, Chen M, Org. Lett 2018, 20, 3810. [PubMed: 29897243]

[8]. a)Reddy LR, Chem. Commun 2012, 48, 9189;b)Wang M,Khan S, Miliordos E, Chen M, Adv. Synth. Catal 2018, 360, 4634.

[9]. a)Grayson MN, Pellegrinet SC, Goodman JM, J. Am. Chem. Soc 2012, 134, 2716; [PubMed: 22239113] b)Wang H, Jain P, Antilla JC,Houk KN, J. Org. Chem 2013, 78, 1208; [PubMed: 23298338] c)Grayson MN,Goodman JM, J. Am. Chem. Soc 2013, 135, 6142; [PubMed: 23517191] d)Grayson MN, Yang Z, Houk KN, J. Am. Chem. Soc 2017, 139, 7717. [PubMed: 28556660]

[10]. a)Gao S, Wang M, Chen M, Org. Lett 2018, 20, 7921; [PubMed: 30543109] b)Wang M, Gao S, Chen M, Org. Lett 2019, 21, 2151; [PubMed: 30864811] c)Chen J,Gao S, Gorden JD, Chen M, Org. Lett 2019, 21, 4638; [PubMed: 31188614] d)Chen J, Gao S, Chen M, Org. Lett 2019, 21, 8800; [PubMed: 31638404] e)Chen J, Gao, Chen M, Org. Lett 2019, 21, 9893; [PubMed: 31793302] f)Gao S, Chen J, Chen M, Chem. Sci 2019, 10, 3637; [PubMed: 30996958] g)Gao S, Chen M, Chem. Sci 2019, 10, 7554; [PubMed: 31489170] h)Gao S, Chen M, Chem. Commun 2019, 55, 11199;i)Liu J, Tong X, Chen M, J. Org. Chem 2020, 85, 5193; [PubMed: 32227947] j)Liu J, Su B, Chen M, Org. Lett 2021, 23, 6035; [PubMed: 34282917] k)Liu J, Gao S, Chen M, Org. Lett 2021, 23, 7808; [PubMed: 34558913] l)Liu J, Gao S, Chen M, Org. Lett 2021, 23, 9451; [PubMed: 34860521] m)Liu J, Chen M, Chem. Commun 2021, 57, 10799;n)Chen J, Miliordos E, Chen M, Angew. Chem. Int. Ed 2021, 60, 840;Angew. Chem 2021, 133, 853.

[11]. a)Kobayashi J, Kubota T, J. Nat. Prod 2007, 70, 451; [PubMed: 17335244] b)Kobayashi J, J. Antibiot 2008, 61, 271;c)Tang Y, Xue Y, Du G, Wang J, Liu J, Sun B, Li X, Yao G, Luo Z, Zhang Y, Angew. Chem. Int. Ed 2016, 55, 4069;Angew. Chem 2016, 128, 4137.

[12]. a)Brown HC, Randad RS, Tetrahedron Lett 1990, 31, 455;b)Brown HC, Randad RS, Tetrahedron 1990, 46, 4463;c)Yu C-M, Jeon M, Lee J-Y, Jeon J, Eur. J. Org. Chem 2001, 1143;d)Xiang M, Luo G, Wang Y, Krische MJ, Chem. Commun 2019, 55, 981;e)Zhang Y-L, He B-J, Xie Y-W, Wang Y-H, Wang Y-L, Shen Y-C, Huang Y-Y, Adv. Synth. Catal 2019, 361, 3074.

[13]. a)Faraldos JA, Giner J-L, J. Org. Chem 2002, 67, 4659; [PubMed: 12098273] b)Chow CP, Shea KJ, Sparks SM, Org. Lett 2002, 4, 2637; [PubMed: 12153197] c)Terauchi T, Tanaka T, Terauchi T, Morita M, Kimijima K, Sato I, Shoji W, Nakamura Y, Tsukada T, Tsunoda T, Hayashi G, Kanoh N, Nakata M, Tetrahedron Lett 2003, 44, 7747;d)Reznik SK, Marcus BS, Leighton JL, Chem. Sci 2012, 3, 3326; [PubMed: 25165502] e)Reznik SK, Leighton JL, Chem. Sci 2013, 4, 1497; [PubMed: 25165503] f)Xu Y, Yin Z, Lin X, Gan Z, He Y, Gao L, Song Z, Org. Lett 2015, 17, 1846; [PubMed: 25825952] g)Zhang Z, Xie H,Li H, Gao L, Song Z, Org. Lett 2015, 17, 4706; [PubMed: 26371396] h)Li L, Sun X, He Y, Gao L, Song Z, Chem. Commun 2015, 51, 14925.

[14]. a)Zanoni G, Castronovo F, Franzini M, Vidari G, Giannini E, Chem. Soc. Rev 2003, 32, 115; [PubMed: 12792935] b)Tanaka T, Hayashi M, Synthesis 2008, 3361;c)Bartók M, Chem. Rev 2010, 110, 1663; [PubMed: 19873975] d)Beletskaya IP, Nájera C, Yus M, Chem. Rev 2018, 118, 5080. [PubMed: 29676895]

[15]. Gao S, Duan M, Houk KN, Chen M, Angew. Chem. Int. Ed 2020, 59, 10540;Angew. Chem 2020, 132, 10627.

[16]. a)Dale JA, Mosher HS, J. Am. Chem. Soc 1973, 95, 512;b)Ohtani I, Kusumi T, Kashman Y, Kakisawa H, J. Am. Chem. Soc 1991, 113, 4092;c)Hoye TR, Jeffrey CS, Shao F, Nat. Protoc 2007, 2, 2451. [PubMed: 17947986]

[17]. For selected examples of enantiodivergent catalysis:a)Nakayama K, Maruoka K, J. Am. Chem. Soc 2008, 130, 17666; [PubMed: 19055327] b)Galván A, González-Pérez AB, Álvarez R, de Lera AR, Fañanás FJ, Rodríguez F, Angew. Chem. Int. Ed 2016, 55, 3428;Angew. Chem 2016, 128, 3489;c)Neel AJ, Milo A,Sigman MS, Toste FD, J. Am. Chem. Soc 2016, 138, 3863; [PubMed: 26967114] d)Mori K, Itakura T, Akiyama T, Angew. Chem. Int. Ed 2016, 55, 11642;Angew. Chem 2016, 128, 11814;e)Macharia J,Wambua V, Hong Y, Harris L, Hirschi JS, Evans GB, Vetticatt M, Angew. Chem. Int. Ed 2017, 56, 8756;Angew. Chem 2017, 129, 8882;f)Chan Y-C, Wang X, Lam Y-P, Wong J,Tse Y-LS, Yeung Y-Y, J. Am. Chem. Soc 2021, 143, 12745. [PubMed: 34350758]

[18]. Gao S, Chen M, Org. Lett 2018, 20, 6174. [PubMed: 30256121]

[19]. a)Ishiyama T, Yamamoto M, Miyaura N, Chem. Commun 1996, 2073;b)Ishiyama T, Yamamoto M, Miyaura N, Chem. Commun 1997, 689;c)Clegg W, Johann TRF, Marder TB, Norman NC, Orpen AG, Peakman TM, Quayle MJ, Rice CR, Scott AJ, J. Chem. Soc. Dalton Trans 1998, 1431.

[20]. Hilt G, du Mesnil F-X, Lüers S, Angew. Chem. Int. Ed 2001, 40, 387;Angew. Chem 2001, 113, 408.

[21]. Kotha S, Chavan AS, J. Org. Chem 2010, 75, 4319. [PubMed: 20496902]

[22]. Curini M, Epifano F, Marcotullio MC, Rosati O, Hetero-cycles 2001, 55, 1599.

[23]. Frisch MJ, et al. Gaussian 16; Revision A.03, Gaussian, Inc., Wallingford, CT, 2016. The full author list is shown in the Supporting Information.

[24]. a)Lee C, Yang W, Parr RG, Phys. Rev. B 1988, 37, 785;b)Stephens PJ, Devlin FJ, Chabalowski CF, Frisch MJ,J. Phys. Chem 1994, 98, 11623;c)Barone V, Cossi M, J. Phys. Chem. A 1998, 102, 1995;d)Cossi M, Rega N, Scalmani G,Barone V, J. Comput. Chem 2003, 24, 669; [PubMed: 12666158] e)Zhao Y, Truhlar DG, Theor. Chem. Acc 2008, 120, 215;f)Zhao Y, Truhlar DG, Acc. Chem. Res 2008, 41, 157. [PubMed: 18186612]

[25]. a)Grimme S, Chem. Eur. J 2012, 18, 9955; [PubMed: 22782805] b)Li Y, Gomes J,Sharada SM, Bell AT, Head-Gordon M, J. Phys. Chem. C 2015, 119, 1840;c)Luchini G, Alegre-Requena JV, Guan Y,Funes-Ardoiz I, Paton RS, 2019, 10.5281/zenodo.595246.

[26]. a)Grimme S, Bannwarth C, Shushkov P, Chem J. Theory Comput 2017, 13, 1989;b)Grimme S, Bannwarth C, Dohm S, Hansen A, Pisarek J, Pracht P, Seibert J, Neese F, Angew. Chem. Int. Ed 2017, 56, 14763;Angew. Chem 2017, 129, 14958;c)Grimme S, Chem J. Theory Comput 2019, 15, 2847;(d)Bannwarth C, Ehlert S, Grimme S, Chem J. Theory Comput 2019, 15, 1652.

[27]. a)Lu T, Chen F, J. Comput. Chem 2012, 33, 580; [PubMed: 22162017] b)Lefebvre C, Rubez G, Khartabil H, Boisson J-C, Contreras-García J, Hénon E, Phys. Chem. Chem. Phys 2017, 19, 17928. [PubMed: 28664951]

[28]. a)Bickelhaupt FM, Houk KN, Angew. Chem. Int. Ed 2017, 56, 10070;Angew. Chem 2017, 129, 10204;b)Duan M, Diaz-Oviedo CD, Zhou Y, Chen X, Yu P, List B, Houk KN, Lan Y, Angew. Chem. Int. Ed 2022, 61, e202113204;Angew. Chem 2022, 134, e202113204.

[29]. Reactions of benzaldehyde with β-methyl, phenyl and Cl-substituted allylboronates gave products with < 10% ee.

[30]. Deposition numbers 2189737 (**2f**), 2189738 (**2i**), 2189733 (**2j**), 2189732 (**2k**), 1875628 (**4b**), 2189741 (**4e**), 2189742 (**4f**) contain the supplementary crystallographic data for this paper. These data are provided free of charge by the joint Cambridge Crystallographic Data Centre and Fachinformationszentrum Karlsruhe Access Structures service.
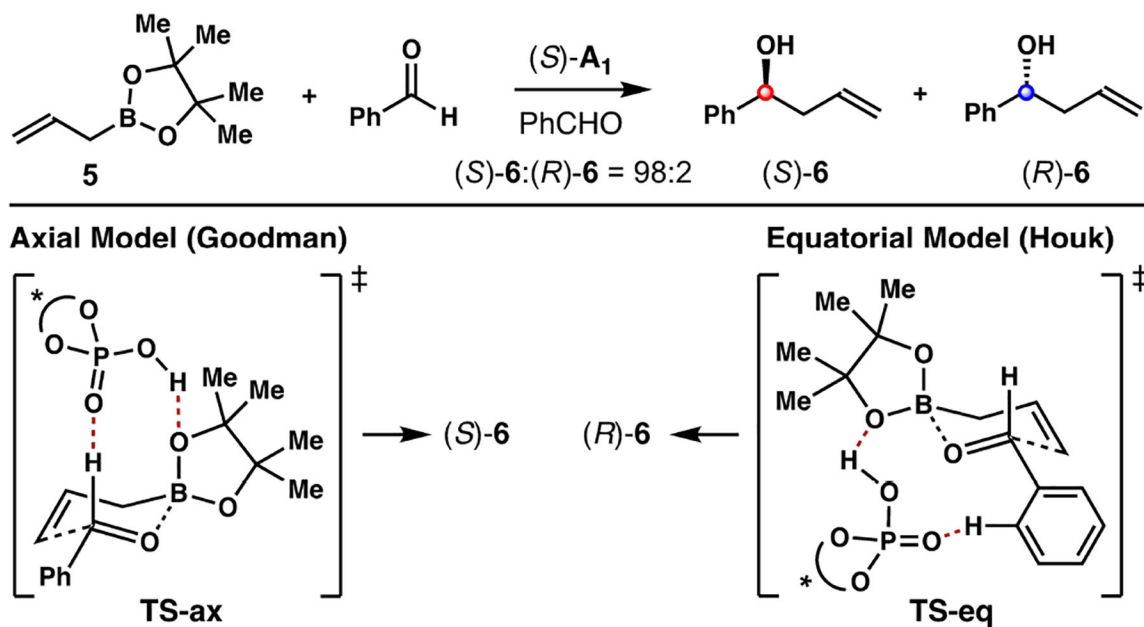
Figure 1.
The axial model (Goodman) and the equatorial model (Houk) for chiral phosphoric acid
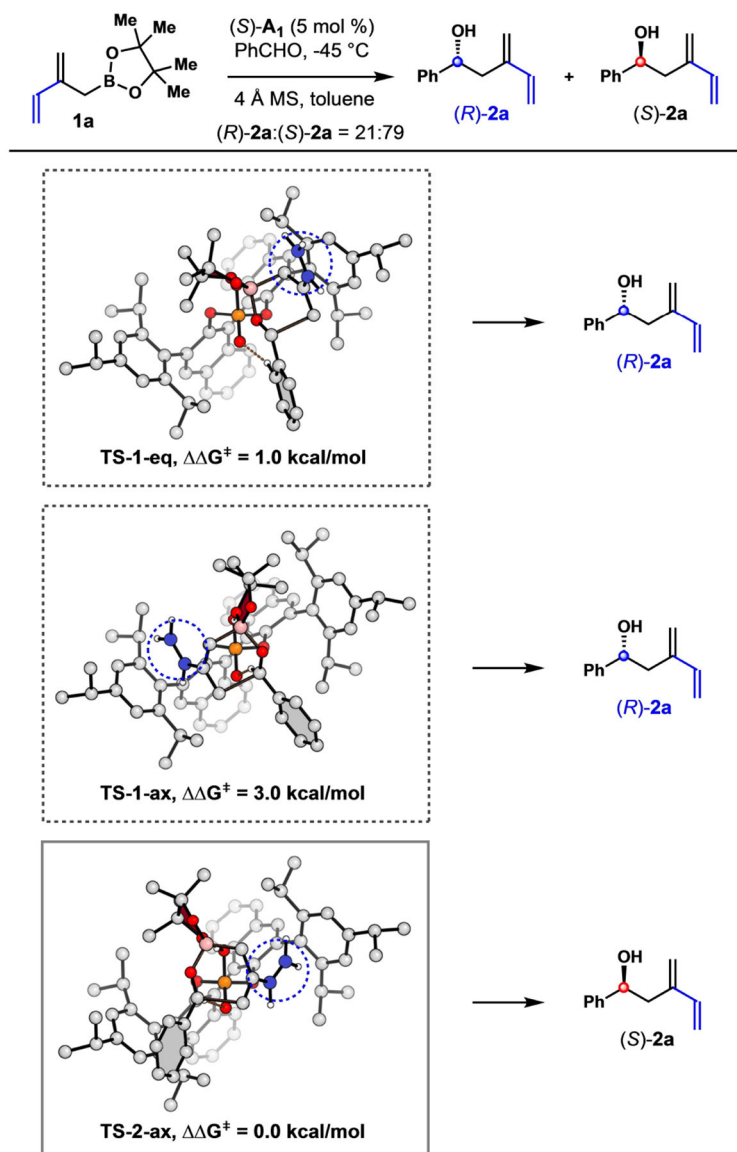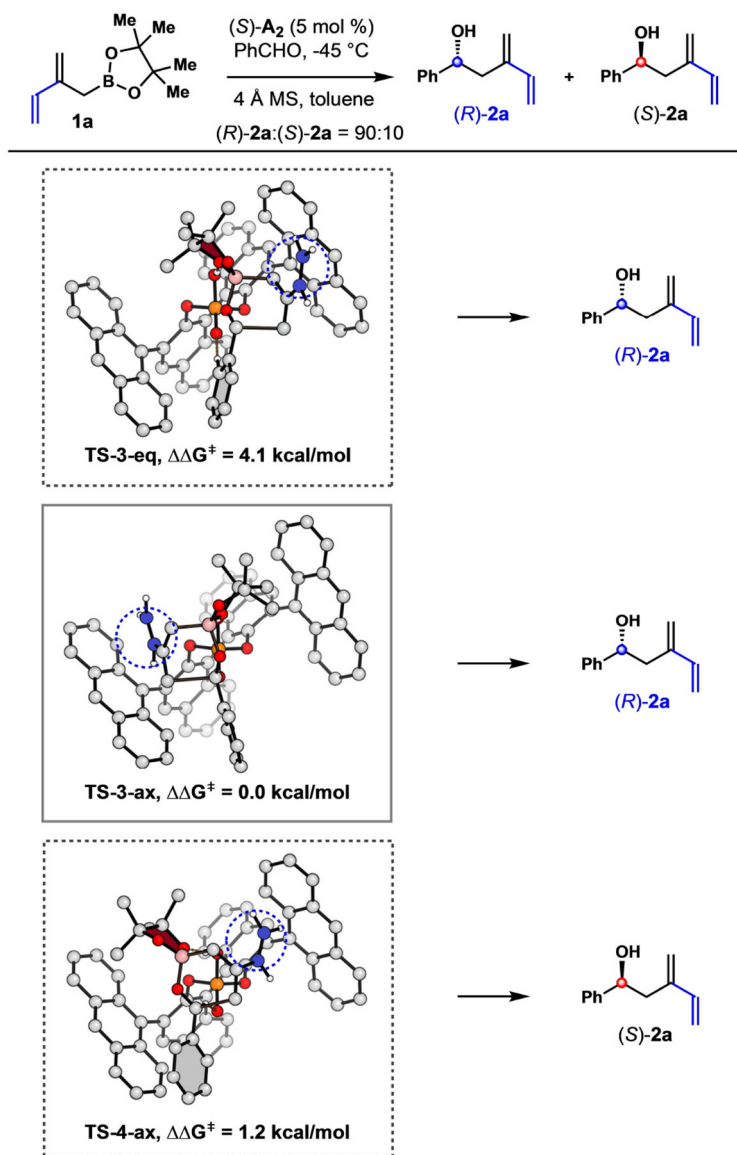(S)-A_1-catalyzed allylboration of benzaldehyde with **5**.

Figure 2.
DFT-optimized transition states **TS-1-eq**, **TS-1-ax**, and **TS-2-ax** of chiral phosphoric acid
(*S*)-**A₁**-catalyzed addition to benzaldehyde with reagent **1a**. Energy differences are given in
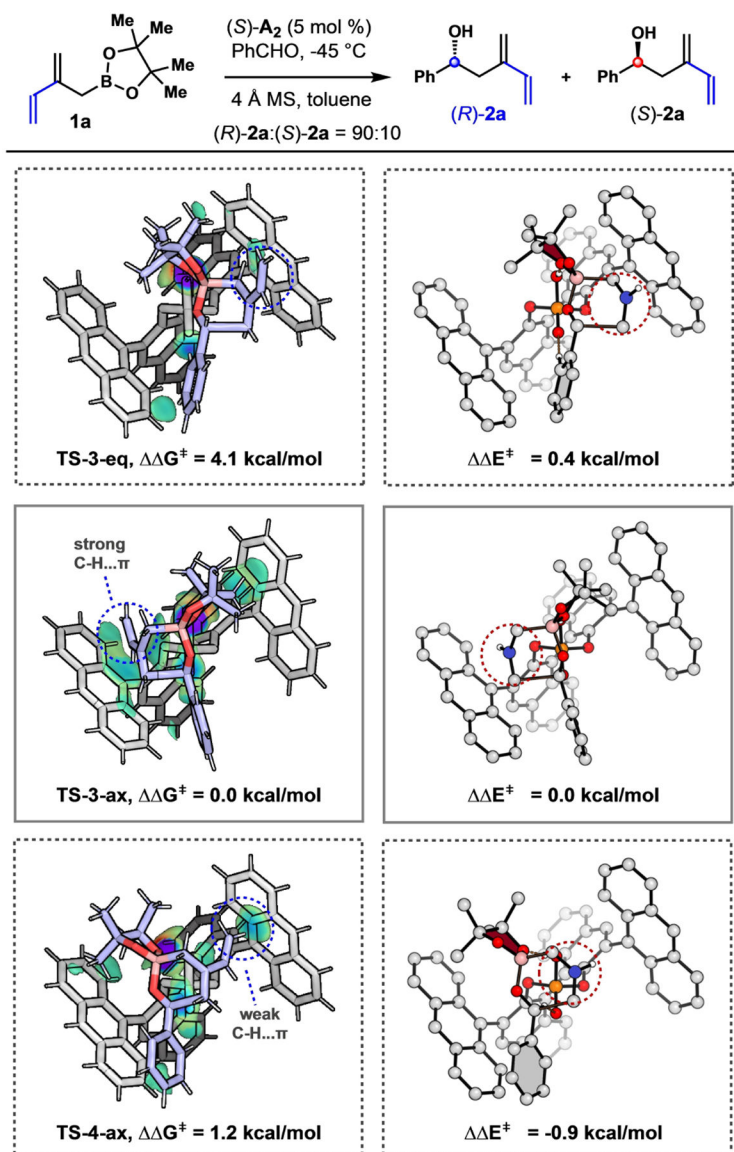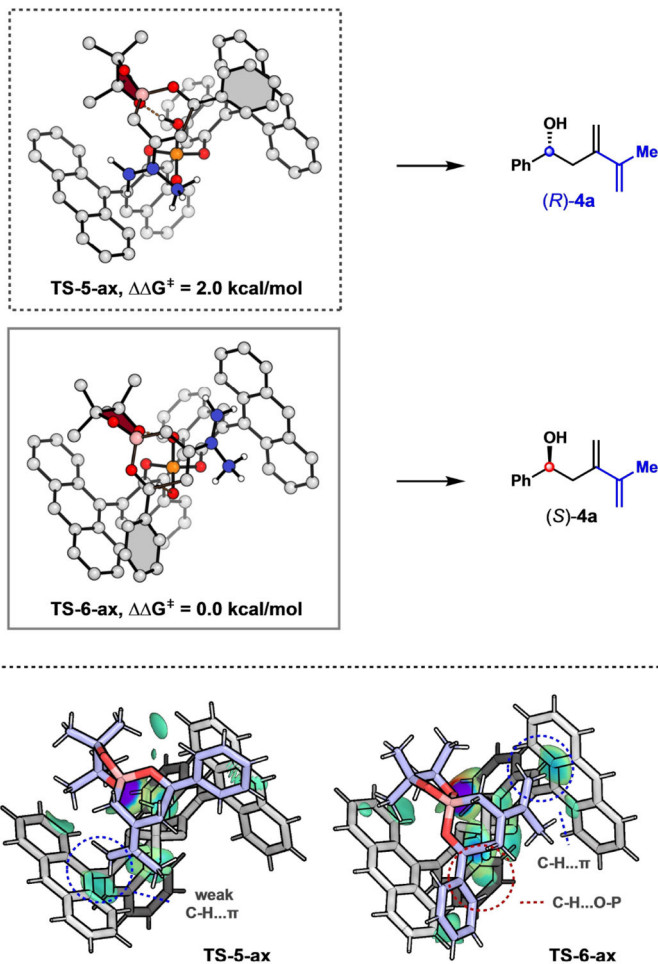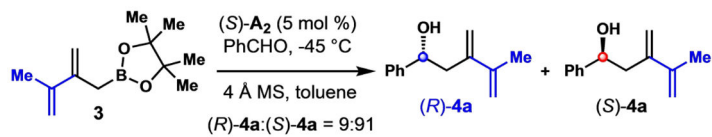kcal mol^{-1}. Non-critical hydrogen atoms in all computed structures are hidden to improve
clarity.

Figure 3.
DFT-optimized transition states **TS-3-eq**, **TS-3-ax**, and **TS-4-ax** of chiral phosphoric acid (*S*)-**A$_2$**-catalyzed addition to benzaldehyde with reagent **1a**. Energy differences are given in kcal mol^{-1}. Non-critical hydrogen atoms in all computed structures are hidden to improve clarity.

Figure 4.
Color-filled NCI isosurfaces of transition states **TS-3-eq**, **TS-3-ax**, and **TS-4-ax** (blue: strong attraction; green: weak interactions; red: steric effect). Right column: single-point calculations by replacing the vinyl group of **1a** with a hydrogen atom. Energy differences are given in kcal mol^{-1}. Non-critical hydrogen atoms in all computed structures are hidden to improve clarity.

Figure 5.
DFT-optimized transition states **TS-5-ax** and **TS-6-ax** of chiral phosphoric acid (S)-**A$_2$**-catalyzed addition to benzaldehyde with reagent **3**. Bottom panel: color-filled NCI isosurfaces (blue: strong attraction; green: weak interactions; red: steric effect). Energy differences are given in kcal mol^{-1}. Non-critical hydrogen atoms in all computed structures are hidden to improve clarity.
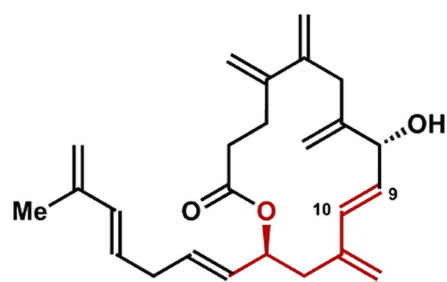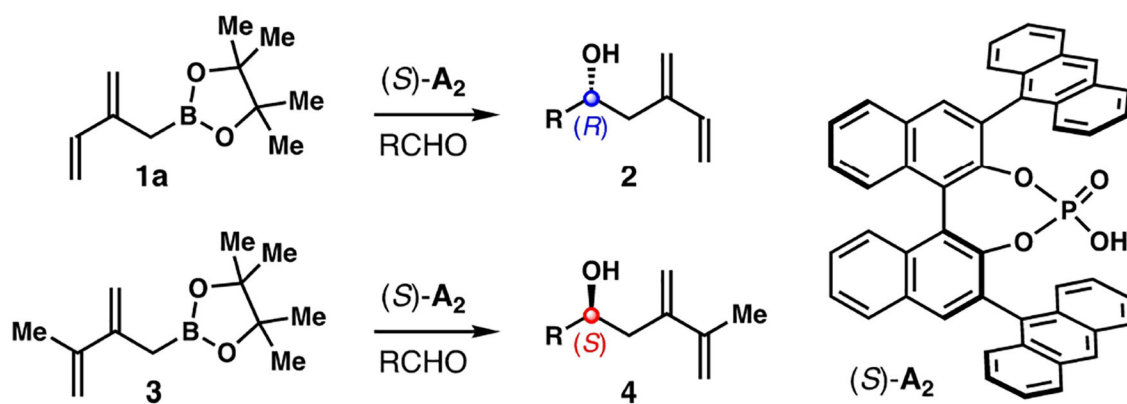
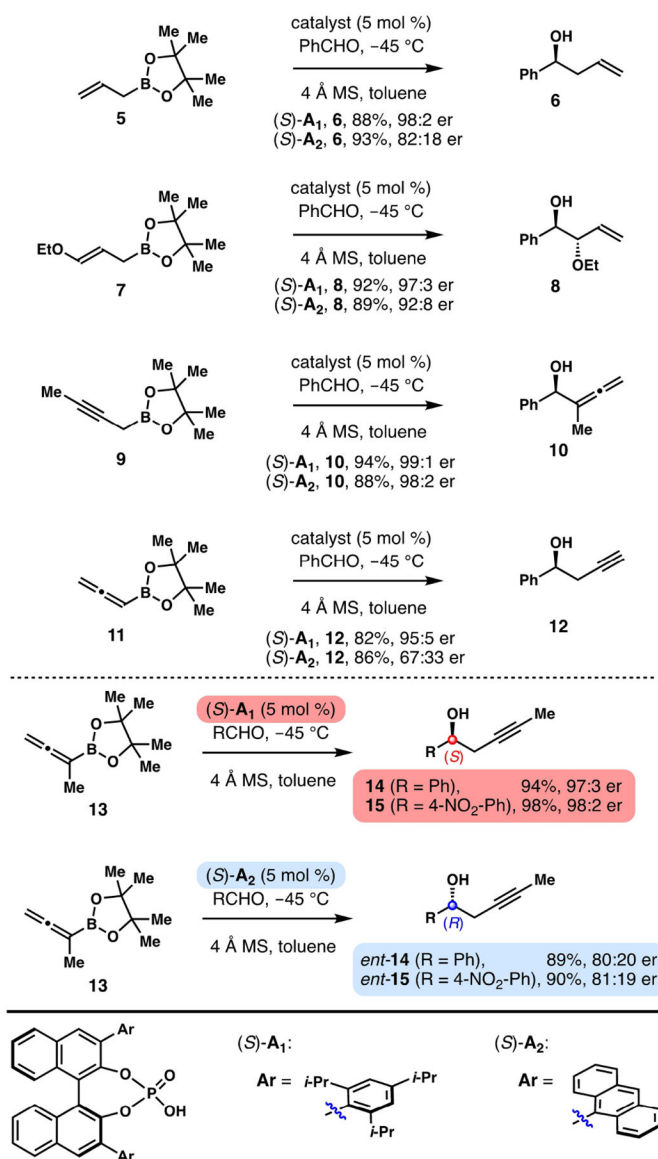9,10-*des*-epoxy-amphidinolide V
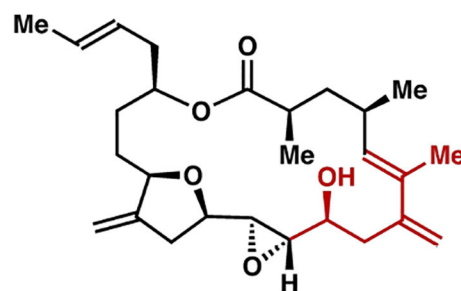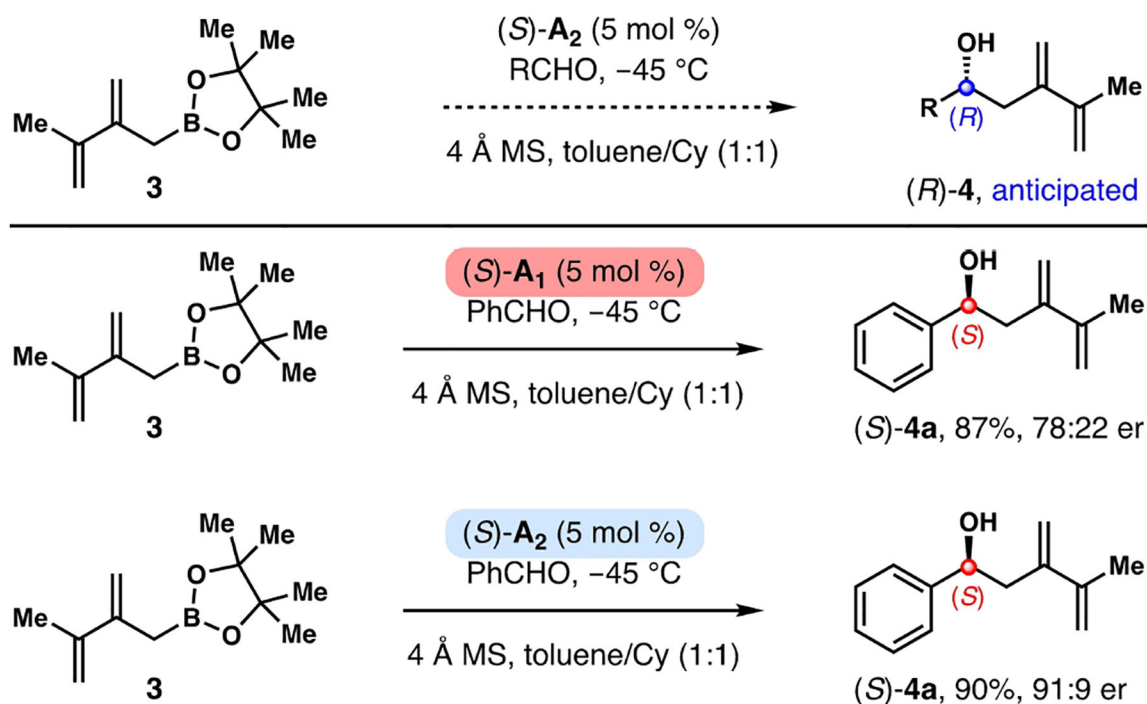
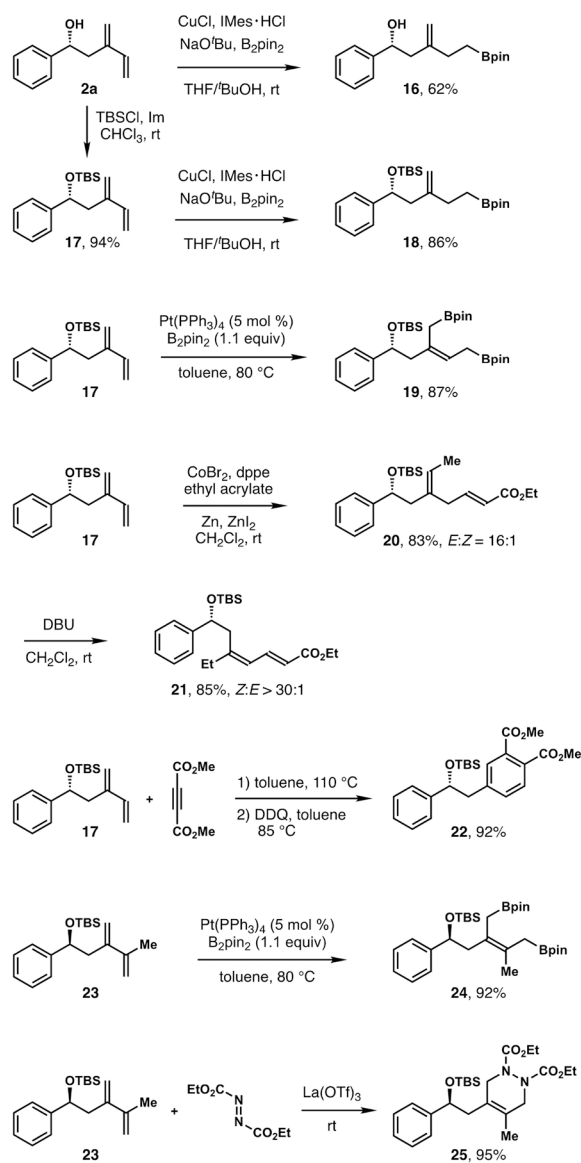amphidinolide K
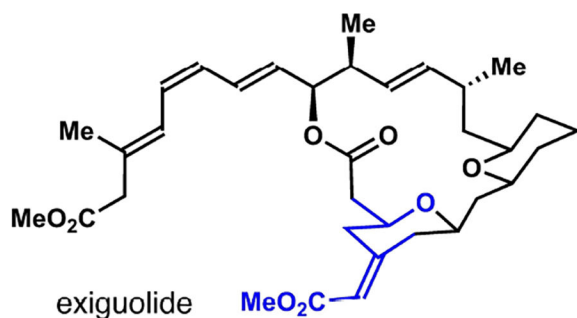
exiguolide
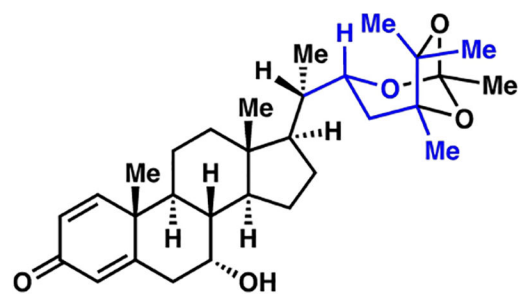
petuniasterone D

Scheme 1.
Proposed approach to γ-alkenyl homoallylic alcohols **2** and **4**.

Scheme 2.
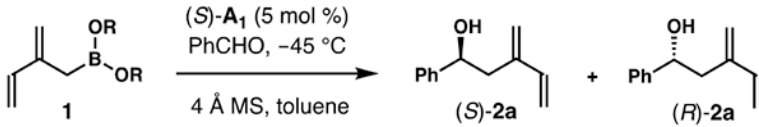Evaluation of the reactions with other unsaturated boron reagents.

Scheme 3.
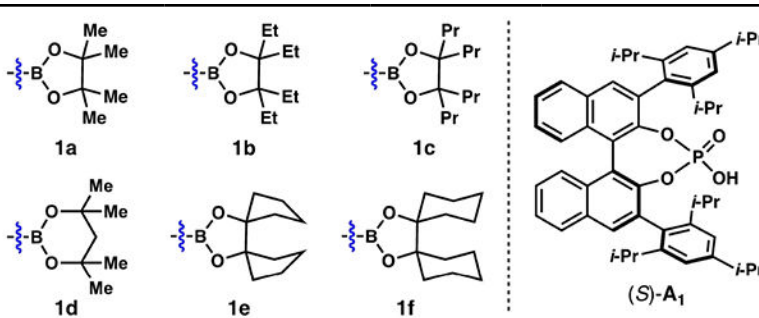Asymmetric aldehyde addition with reagent **3**.

Scheme 4.
Derivatization of reaction products.

Table 1:

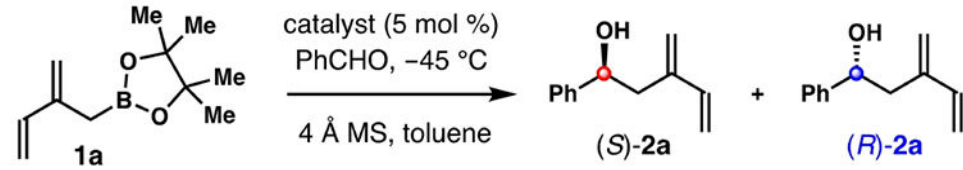Initial studies with allylboronates **1** bearing different diol groups.[a–c]

entry	boronate	yield	(*S*)-2a:(*R*)-2a
1	**1a**	86%	79:21
2	**1b**	98%	72:28
3	**1c**	75%	70:30
4	**1d**	92%	68:32
5	**1e**	80%	63:37
6	**1f**	86%	55:45

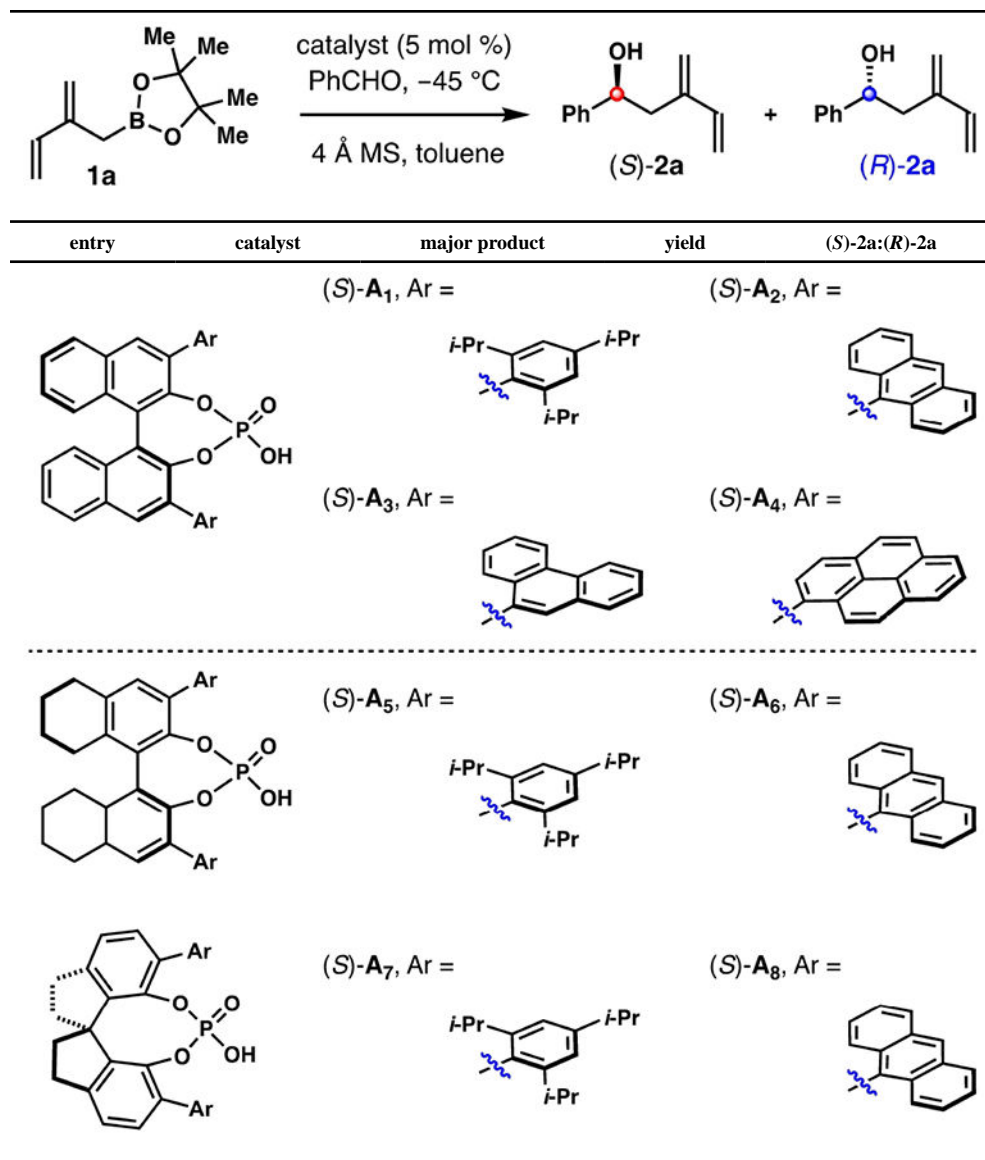[a]Boronate **1** (0.12 mmol, 1.2 equiv), benzaldehyde (0.1 mmol,1.0 equiv), (S)-**A₁** (5 mol %), 4 Å molecular sieves (50 mg), toluene, –45 °C.

[b]Yields of isolated products are listed.

[c]Enantioselectivities were determined by HPLC analysis.

Table 2:

Optimization of the chiral phosphoric acid catalyst.[a–f]

entry	catalyst	major product	yield	(S)-2a:(R)-2a
1	(S)-A_1	(S)-2a	86%	79:21
2	(S)-A_2	(R)-2a	98%	10:90
3	(S)-A_3	(S)-2a	92%	52:48
4	(S)-A_4	(S)-2a	80%	53:47
5	(S)-A_5	(S)-2a	86%	84:16
6	(S)-A_6	(R)-2a	92%	23:77
7	(S)-A_7	(S)-2a	86%	81:19
8	(S)-A_8	(R)-2a	80%	24:76
9[e]	(S)-A_2	(R)-2a	86%	25:75
10[f]	(S)-A_2	(R)-2a	92%	7:93

[a] Reaction conditions: boronate **1a** (0.12 mmol, 1.2 equiv), benzaldehyde (0.1 mmol, 1.0 equiv), phosphoric acid (5 mol %), 4 Å molecular sieves (50 mg), toluene (0.3 mL), −45 °C, 48 h.

[b] Yields of isolated products are listed.

[c] The absolute configuration of the hydroxyl group in **2** was established by Mosher ester analyses.

[d] Enantiomeric ratios were determined by HPLC analysis.

[e] The reaction was conducted without 4 Å molecular sieves.

[f] The reaction was conducted in toluene/cyclohexane (1:1). Cy: cyclohexane.

Table 3:

Scope of aldehyde for reactions with boronate **1a** catalyzed by (S)-**A$_2$**.

Table 4:

Aldehyde scope for (S)-**A₂**-catalyzed reactions with boron reagent **3**.[a–c]